Proceedings of ASME 2016 Summer Heat Transfer Conference
SHTC16
July 10-14, 2016, Washington, DC, USA

HT2016-7188

CRYOGENIC TEMPERATURE MONITORING VIA OPTICAL PDMS SENSORS

Matthew Frenkel
Dept. of Mechanical and Aerospace Engineering
Rutgers University
Piscataway, NJ 08854, USA

Zhixiong Guo
Dept. of Mechanical and Aerospace Engineering
Rutgers University
Piscataway, NJ 08854, USA

ABSTRACT
PDMS micro-sensors coated onto an electrical wire are used to measure dynamic temperature variation at cryogenic range based on optical whispering-gallery mode (WGM) frequency shift principle. We designed a lab cryogenic cell via filling liquid nitrogen to create a stable low temperature down to 95K. The electrical wire is current carrying to simulate a working electrical/electronic component/device. The temperature variation due to Joule heating is monitored. The sensors are tested for their real time temperature monitoring capabilities and accuracy in the cryogenic temperature regime of 95 – 140K.

INTRODUCTION
Optical whispering-gallery mode (WGM) studies have attracted considerable attention over the past two decades (1-5). The small mode volume, localized to the surface, of optical WGM resonators (1,2) allows for considerable interaction with surrounding environment, and their intrinsically high quality (Q) factor enables WGM-based sensors to exhibit extremely high-resolution. Optical WGM sensors are being actively studied in a number of different detection and measurement applications. Examples included biological/chemical detection (3-8), humidity (9), pressure (10) and temperature (11-13) monitoring, to name a few. The intrinsic high Q-factor of WGM based sensors, in junction with the fact that the sensing principles are frequency, and not intensity based, enables high sensitivity and fine resolution measurement. Detection of single molecule and individual RNA viruses (4,5), pico-molar chemical residues (8), milli-newton force (10), and milli-kelvin temperature shifts (12) have been reported in the literature.

Optical WGM temperature sensors were initially demonstrated at both room temperature (11, 12) and cryogenic (13) regimes using fused silica microspheres. He *et al*. (14) analyzed thermal compensation in WGM resonators coated with a layer of polydimethylsiloxane (PDMS). Several studies of PDMS coating on thermal sensing then followed (15-17). Li *et al*. (16) proposed the concept of on-chip sensing based on WGM resonance. The actual demonstration of on-chip dynamic temperature measurement was carried out by Frenkel *et al*. (17), in which a PDMS based WGM resonator was fabricated directly onto an electrical current-carrying wire and be used for dynamic temperature monitoring of the wire's temperature due to Joule heating. WGM resonances of the coated PDMS composite sensors were determined jointly by the thermal effects of both the PDMS shell and core material. Recently, Ali *et al.* (18) considered polymeric microspheres to electrical field measurement.

In this paper, we look to expand on our previous work with PDMS composite sensors at room temperature (17) to cryogenic temperature because of wide cryogenic applications. For example, it is paramount to determine the critical temperature of superconductivity. Because of the ease in fabrication and cost-effectiveness using PDMS coated sensors, it is worthy of exploring the feasibility and capability of PDMS based WGM resonators within the cryogenic temperature regime.

EXPERIMENTAL SETUP
The experimental setup used in this study is adapted from a previous study of the present authors (17). The setup consists of five key components: the working electric component, the WGM composite sensor, the purging chamber, the cryogenic working cell, and the data acquisition system. The working electric component, fabrication of PDMS coated WGM sensor, and data acquisition system were detailed in Frenkel *et al.* (17); the only notable difference, among these three components, is that the fiber taper used as the near-field coupling device was fabricated outside the purging system using the heat and pull method (12). The fabrication was done on a rail system so that it could be transported into the purging chamber without breaking the fragile fiber taper. The reason behind using the rail system instead of fabricating directly within the purging chamber was that the stepper motor could not be placed within the chamber making it more difficult to control the tension

within the fiber taper during fabrication. The lack of tension control could lead to large inconsistencies when creating the fiber taper, and often resulted in huge signal loses when the system was cooled to cryogenic temperatures, sometimes to the point where no signal could be detected by the photo detector. Figure 1 shows the present experimental setup.

The purging chamber and working cell were added to the present experimental setup so that cryogenic temperatures could be reached and the WGM sensor would not undergo any frosting. The purging chamber was built from PVC boards. The chamber base has regularly spaced threaded holes allowing for the mounting of the fiber taper rail system, stages, and posts, as required. The walls of the chamber are lined with a number of threaded ports allowing for whatever gauges and liquid/gas/electrical/optical inlets and outlets the experiment may require. For example, there are two ports used for the optical fiber input/output, one port used for a vacuum gauge, one port attached to a roughing pump, one port used for the liquid nitrogen (LN2) inlet, one port used for the nitrogen gas inlet, one port used for electrical inputs, and one port used for thermocouple inlets, in the present setup. The top of the chamber consists of an O-ring to allow for a vacuum seal, and the PVC lid is attached to the chamber using a number of metal clamps.

The working cell was designed for the purpose of cooling the electrical component to cryogenic temperatures, as well as, to insulate the environment around the WGM resonator eliminating any significant temperature fluctuations caused by air currents around the resonator. To achieve this the working cell was fabricated out of a hollow aluminum bar and covered with insulation. The inside of the aluminum is used as an LN2 reservoir. Two copper rods are inserted into the LN2 reservoir. The electrical component is threaded through holes in these rods allowing them to act as cold fingers. Two steel screws are also threaded through the aluminum, the electrical component is tied around these two screws, and they can be adjusted to control tension in the electrical component as well as alignment between the WGM sensor and the fiber taper. A combination of electrical tape and thermal paste is used to electrically insulate the electrical component form the rest of the system, while keeping it in good thermal contact. The WGM sensor is surrounded by a larger solid piece of copper that also reaches into the LN2 reservoir. This piece of copper has two perpendicular channels machined into it to allow both the fiber taper and electrical component to be positioned inside of it, the purpose of this copper is to increase the thermal inertia around the resonator allowing a more stable thermal environment at cryogenic temperatures. A second thin walled copper cylinder surrounds this piece of copper; this thin walled copper has 4 slits roughly one millimeter thick cut into it. These slits line up with the channels in the larger copper cylinder and prevent any air currents from affecting the thermal stability around the WGM sensor. A PDMS lid covers the larger copper cylinder. An additional aluminum case is placed around the entire electrical component, copper, and aluminum rods, and covered

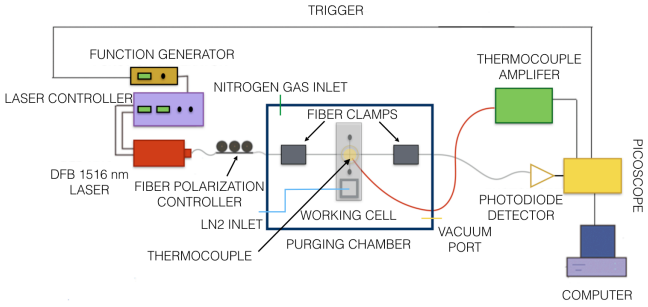

FIGURE 1. EXPERIMENTAL SETUP.

with a PDMS lid, to allow for additional insulation of the cryogenic environment, several small holes were drilled into this casing so that thermocouples can be used to monitor the temperatures of the cold fingers and WGM sensor environment. Figure 2 shows both a cross section and a top view of the working cell.

Lastly, PDMS was chosen instead of fused silica as the WGM resonator medium primarily because of its ease in fabrication. PDMS coated WGM resonators can be fabricated at room temperature using techniques put forth in Frenkel *et al.* (17), where as, fused silica WGM resonators require temperatures that would ignite the nichrome wire used as the electrical component, and would cause failure in most other materials that could be used to replace the nichrome, such as tungsten. This does have some drawbacks. PDMS will have a lower *Q*-factor than a fused silica resonator due to intrinsic material properties and surface smoothness. PDMS has, to the author's knowledge, not been explored as a WGM resonator at cryogenic temperatures, therefore it was unknown if a PDMS resonator would support WGMs in the desired temperature range.

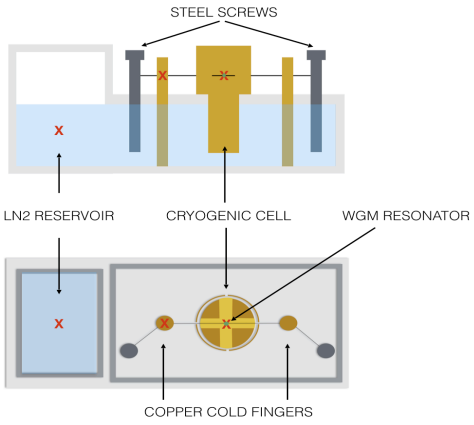

FIGURE 2. CROSS-SECTIONAL AND TOP VIEWS OF THE CRYOGENIC WORKING CELL, THE RED X'S REPRESENT THERMOCOUPLE LOCATIONS.

RESULTS AND DISCUSSION

Before experiments with WGM sensors could take place, the low temperature capabilities and stability of the working cell needed to be determined. It was found that when the LN2 reservoir was filled, normally taking about 4 liters of LN2 slowly poured through the LN2 outlet over the course of 20 to 25 minutes that a stable < 90K could be reached in the cold fingers, and a stable temperature < 100K could be reached within the cryogenic working cell. The LN2 reservoir was capable of keeping the system at these low temperatures for approximately 10 minutes before it was depleted enough to allow the system to warm. Figure 3 shows the temperatures curves of the LN2 reservoir, one cold finger, and within the cryogenic cell during the cooling, stable, and warming processes. The positions of these thermocouples are marked with red X's in figure 2. It can also be seen that a vacuum was introduced into the system shortly after the LN2 reservoir was filled. The intention of this vacuum was to cause a phase change of the LN2 into solid nitrogen dropping its temperature an additional 5-10K. It can be seen that both the LN2 reservoir and the cold finger responded to this vacuum with temperature drops, but that the temperature within the cryogenic cell began to warm slightly under the vacuum. We attribute this warming within the cryogenic cell to the influx of the warmer surrounding air contained within the purging chamber that will occur because of the pressure differential created by the roughing pump. This warming could be overcome with a larger LN2 reservoir that would give the system more time to reach equilibrium with the solid nitrogen under vacuum, but such a reservoir is currently incompatible with the dimensions of our purging chamber, therefore, no vacuum was used when testing the WGM sensors. It was also found that if the system was cooled and left to warm without any vacuum the temperature within the cryogenic cell changed < 1K throughout the stable region of the temperature profile.

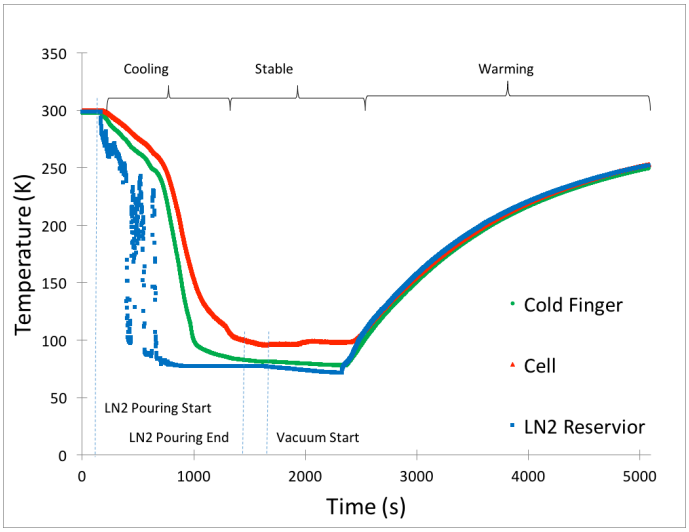

FIGURE 3. TEMPERATURE PROFILES OF VARIOUS PARTS OF THE WORKING CELL.

The first WGM experiments conducted were meant to determine if PDMS was capable of supporting WGM resonance at cryogenic temperatures. The working cell was cooled as previously described. Prior to the cooling of the working cell the purging chamber underwent a nitrogen gas purging. The purpose of this nitrogen purge is to remove any humidity contained within the chamber, and thus prevent any frosting that could occur on the resonator or fiber taper. If frosting were allowed to occur, it would affect the coupling between the resonator and taper either decoupling the system completely or reducing the signal received by the photo-detector beyond detection. While the system is being cooled after the nitrogen purge, the WGM signal can be watched on a local computer. A decrease in signal was often seen accompanying the system cooling. This decrease in signal can most likely be attributed to tension created in the fiber taper due to the thermal strain placed on it. The signal loss was normally on the order of ~20dB and could be easily made up for with the gain of the photo-detector, unlike the signal loss that occurred without a nitrogen purge. Additionally, a drop in resonator quality was also seen as the system was cooled. This drop was normally smaller than an order of magnitude and may be a result of changes in the optical and surface properties of the PDMS as it is cooled. At cryogenic temperature Q-factors of the PDMS resonators were often found around ~1.5 x 10^5 down from values around ~5 x 10^5 at room temperature.

Once the system reached a stable temperature data could be collected as the system warmed naturally. Using the same procedure as discussed in Frenkel *et al.* (17) data was collected at regular intervals throughout the warming of the system. This data could be used to calibrate the sensitivity of the PDMS WGM resonator at cryogenic temperatures. Figure 4 shows a single calibration curve for a 639μm in diameter PDMS shell resonator, fabricated by allowing a PDMS droplet (10:1 weight ratio base to curing agent) to cure onto the nichrome wire (127μm in diameter). The curve shows a linear relationship (R^2 = 0.9985) between temperature shifts and wavelength shifts from temperature of approximately 95K to 140K. The value of the sensitivity is 0.0214nm/K. This value is of interest because it demonstrates a clear difference from the expected room temperature sensitivity. Frenkel *et al.* (17) showed that a PDMS coated resonator of this size, at room temperature should have a sensitivity between 0.1 and 0.15nm/K. Therefore, it is clear that the optical and thermal properties of the PDMS and nichrome have changed when cooled to cryogenic temperatures.

After calibrating a resonator, we were able to perform dynamic temperature monitoring by introducing an electrical current into the nichrome wire. Two probes are connected to the electrical wire between the steel screws and copper cold finger on both sides of the working cell allowing a current to travel along this component and introduce joule heating into the system. The PDMS shell resonator can then be used to directly monitor the temperature of the heating wire in real time. Figure 5 shows the heating curves at three different currents (0.0375A, 0.043A, 0.052A). The electrical current is introduced into the

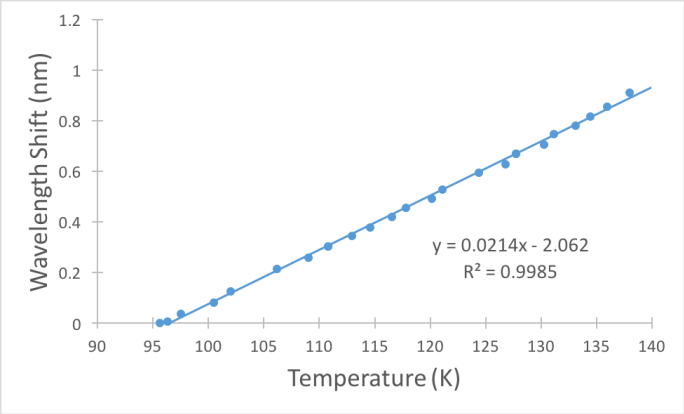

FIGURE 4. A SINGLE CALIBRATION SHOWING TEMPERATURE VS WAVELENGTH SHIFTS FROM 95 TO 140K

system after a few seconds after data acquisition begins, at which point we see the expected heating curve for a wire undergoing internal Joule heating. Again, without the thermal properties of PDMS and nichrome in this temperature range, we cannot conduct a full dynamic theoretical analysis of the heated system. On the other hand, a steady-state theoretical analysis can be preformed by setting the internal energy generated within the wire to the energy dissipated to ambient by convection. A simple energy balance of the system yields equation (1):

$$\frac{4I^2\sigma_e}{\pi D_1^2} = \pi D_2 h \Delta T \tag{1}$$

where I is the current, ΔT is the change in temperature, h is the convective heat transfer coefficient due to natural convection in the ambient, and σ_e is the electrical resistivity of the nichrome core. For the cryogenic temperature range 95-140K, the averaged resistivity of the nichrome wire was found to be 1.261 ± 0.08Ωμm. The convective heat transfer coefficient was determined via Churchill and Chu's correlation for natural convection over a horizontal cylinder (19):

$$\frac{hD_2}{k} = \left\{0.6 + \frac{0.387Ra_D^{1/6}}{\left[1+(0.559/Pr)^{9/16}\right]^{8/27}}\right\}^2 \tag{2}$$

In which, Pr is the Prandtl number, Ra_D is the Rayleigh number, and k is the thermal conductivity of the fluid. This approximation is valid for $10^{-5} < Ra_D < 10^{12}$. Both the Prandtl and Rayleigh numbers where calculated assuming a pure nitrogen gas environment at approximately 100K. At this temperature and in this system Pr = 0.76 and the Rayleigh number is found to be between approximately 0.15 and 0.28 depending on the temperature shift. Table 1 compares the temperature rises in steady state between theoretical analysis and experimental measurement. The error for the theoretical prediction is based on error propagation from the measurements of the core and coating diameters, as well as, the measurements of electrical resistivity and current. Our experimental and theoretical data are in excellent agreement.

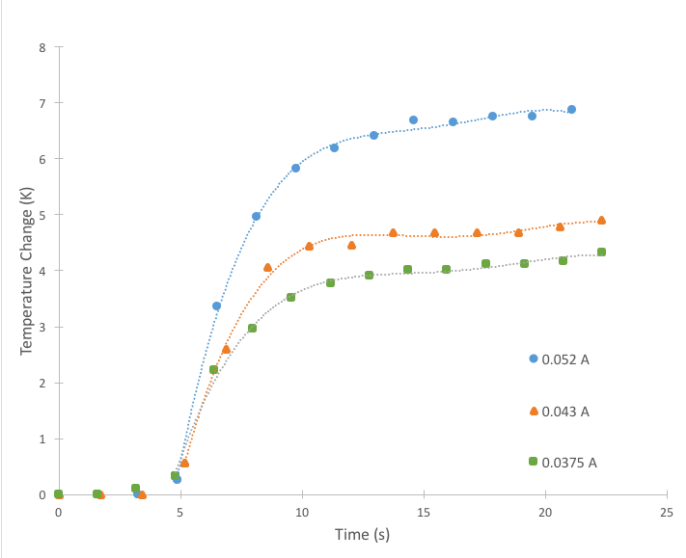

FIGURE 5. REAL TIME TEMPERATURE MONITORING PREFORMED BY A CALIBRATED WGM RESONATOR AT 3 DIFFERENT ELECTRICAL CURRENTS AND FITTING LINES.

CONCLUSIONS

The results of this study demonstrate that PDMS coated micro-resonators will support WGM resonance at cryogenic temperatures, and that these polymeric composite sensors can be used to accurately monitor on-chip temperature changes in cryogenic environment. We built a simple cryogenic system capable of reaching a stable temperature down to 95K. At this temperature the PDMS coated sensors were calibrated to obtain their sensitivities. The polymeric sensors achieved Q-factors on the order of 10^5, resulting in a fine temperature resolution 0.01K at the cryogenic regime. The temperature rising in the current-carrying wire was monitored by the coated PDMS sensor, such that on-site dynamic information was acquired. The comparison of measurement with theoretical analysis showed an excellent agreement.

TABLE 1. COMPARISON OF EXPERIMENTALLY DETERMINED AND THEORETICALLY PREDICT TEMPERATURE RISES AT STEADY STATE.

Current (A)	Experimental ΔT (K)	Analytical ΔT (K)	Difference (K)
0.0375	4.11 ± 0.12	3.84 ± 0.52	0.27
0.043	4.83 ± 0.13	4.86 ± 0.64	0.03
0.052	6.79 ± 0.14	6.76 ± 0.86	0.03

ACKNOWLEDGMENTS

This material is based upon work supported by the National Science Foundation under grant no. CBET-1067141. We

would like to thank Marlon Avellan, John Petrowski, and Joseph Vanderveer whose assistance was instrumental to all the machining needed to fabricate the purging chamber and working cell. M. Frenkel acknowledges partial support of NJSGC Graduate Fellowship 2014-2015.

REFERENCES

1. Dubreuil, N., Knight, J. C., Leventhal, D. K., Sandoghdar, V., Hare, J., and Lefèvre, V., 1995, "Eroded monomode optical fiber for whispering-gallery mode excitation in fused-silica microspheres." Opt. Lett. **20**, pp. 813-815

2. Serpengüzel, A., Griffel, G., and Arnold, S., 1995, "Excitation of resonances of microspheres on an optical fiber." Opt. Lett. **20**, pp. 654-656.

3. Arnold, S., Khoshsima, M., Teraoka, I., Holler, S., and Vollmer, F., 2003, "Shift of Whispering-Gallery Modes in Microspheres by Protein Adsorption." Opt. Lett. **28**, pp. 272-274.

4. Quan, H. and Guo, Z., 2007, "Simulation of Single Transparent Molecule Interaction with Optical Microcavity." Nanotechnology **18**, 375702.

5. Vollmer, F. and Arnold, S., 2008, "Whispering-Gallery-Mode Biosensing: Label-Free Detection Down to Single Molecules." Nature Methods **5**, pp. 591 - 596.

6. He, L., Ozdemir, S. K., Zhu, J., Kim, W. and Yangm L., 2011, "Detecting Single Viruses and Nanoparticles using Whispering Gallery Microlasers." Nature Nanotechnology **6**, pp. 428-432.

7. Dantham, V., Holler, S., Kolchenko, V., Wan, Z., and Arnold, S., 2012, "Taking Whispering Gallery-Mode Single Virus Detection and Sizing to the Limit." Appl. Phys. Lett. **101**, 043704.

8. Huang, L. and Guo, Z., 2012, "Nanofiltration and Sensing of Picomolar Chemical Residues in Aqueous Solution Using Optical Porous Resonator in Microelectrofluidic Channel." Nanotechnology **23**, 065502.

9. Ma, Q., Huang, L., and Guo, Z., 2010, "Spectral Shift Response of Optical Whispering-Gallery Modes Due to Water Vapor Adsorption and Desorption." Meas. Sci. Technol. **21**, 115206.

10. Ioppolo, T., Kozhevnikov, M., Stepaniuk, V., Otugen, M., and Sheverev, V., 2008, "Micro-optical force sensor concept based on whispering gallery mode resonators." App. Opt. **47**, pp. 3009-3014.

11. Guan, G., Arnold, S., and Otugen, V., 2006, "Temperature measurements using a microoptical sensor based on whispering gallery modes." AIAA J **44**, pp. 2385-2389.

12. Ma Q., Rossmann T., and Guo Z., "Temperature sensitivity of silica micro-resonators." J. Phys. D. App. Phys. **41**, 245111 (2008).

13. Ma, Q., Rossmann, T. and Guo, Z., 2010, "Whispering-Gallery Mode Silica Microsensors for Cryogenic to Room Temperature Measurement." Meas. Sci. Technol. **21**, 025310 .

14. He, L., Xiao, Y. F., Dong, C., Zhu J., Gaddam V., and Yang L., 2008, "Compensation of Thermal Refraction Effect in High-Q Toroidal Microresonator by Polydimethylsiloxan Coating." App. Phys. Lett. **93**, 201102.

15. Dong, C. H., He, L., Xiao, Y. F., Gaddam, V. R., Ozdemir, S. K., Han, Z. F., Guo, G. C., Yang, L., 2009, "Fabrication of High-Q Polydimethylsiloxane Optical Microspheres for Thermal Sensing." App. Phys. Lett. **94**, 231119.

16. Li, B., Wang, Q., Xiao, Y., Jiang, X., and Li, Y., C., 2010, "On Chip, High-Sensitivity Thermal Sensor Based on High-Q Polydimethylsiloxane-Coated Microresonator." App. Phys. Lett. **96**, 251109.

17. Frenkel, M., Avellan, M., and, Guo, Z., 20103, "Whipering-Gallery Mode Composite Sensors for On-Chip Dynamic Temperature Monitoring." Meas. Sci. Technol., **24**, 075103.

18. Ali, A.R., Ioppolo, T., Otugen, V., Christensen, M., MacFarlane, D., 2014, "Photonic electric field sensor based on polymeric microspheres". *J. Polymer Sci. B: Polymer Phys.* **52** (3), pp. 276-279.

19. Bejan, A., 2004, Convection Heat Transfer 3rd ed, Wiley, Hoboken, NJ, Chap. 4.

